Ups1p, a conserved intermembrane space protein, regulates mitochondrial shape and alternative topogenesis of Mgm1p

Hiromi Sesaki,[1] Cory D. Dunn,[1] Miho Iijima,[1] Kelly A. Shepard,[2] Michael P. Yaffe,[2] Carolyn E. Machamer,[1] and Robert E. Jensen[1]

[1]Department of Cell Biology, The Johns Hopkins University School of Medicine, Baltimore, MD 21205
[2]Division of Biology, Section of Cell and Developmental Biology, University of California, San Diego, La Jolla, CA 92093

Mgm1p is a conserved dynamin-related GTPase required for fusion, morphology, inheritance, and the genome maintenance of mitochondria in *Saccharomyces cerevisiae*. Mgm1p undergoes unconventional processing to produce two functional isoforms by alternative topogenesis. Alternative topogenesis involves bifurcate sorting in the inner membrane and intramembrane proteolysis by the rhomboid protease Pcp1p. Here, we identify Ups1p, a novel mitochondrial protein required for the unique processing of Mgm1p and for normal mitochondrial shape. Our results demonstrate that Ups1p regulates the sorting of Mgm1p in the inner membrane. Consistent with its function, Ups1p is peripherally associated with the inner membrane in the intermembrane space. Moreover, the human homologue of Ups1p, PRELI, can fully replace Ups1p in yeast cells. Together, our findings provide a conserved mechanism for the alternative topogenesis of Mgm1p and control of mitochondrial morphology.

Introduction

Mitochondrial morphology is essential for the functions of the organelle. Mitochondria fuse and divide in highly regulated manners, and these two activities play a central role in morphogenesis of mitochondria (Jensen et al., 2000; Karbowski and Youle, 2003). Many components involved in mitochondrial fusion and division are highly conserved in a variety of organisms ranging from yeast to humans (Chen and Chan, 2004; Okamoto and Shaw, 2005). Among them, Mgm1p is a conserved dynamin-related GTPase essential for fusion, morphology, inheritance, and the genome maintenance of mitochondria in yeast (Jones and Fangman, 1992; Shepard and Yaffe, 1999; Sesaki et al., 2003b; Wong et al., 2003). Mutations in the human homologue of Mgm1p, OPA1, are linked to autosomal dominant optic atrophy (Alexander et al., 2000; Delettre et al., 2000). There are two species of Mgm1p, an 84-kD form (s-Mgm1p) and a 97-kD form (l-Mgm1p) (Shepard and Yaffe, 1999). These two isoforms exert partially overlapping but distinct functions. Both forms are required for mitochondrial morphology and mitochondrial DNA (mtDNA) maintenance, whereas only l-Mgm1p is required for mitochondrial fusion (Herlan et al., 2003; McQuibban et al., 2003; Sesaki et al., 2003a). In addition, these two isoforms have distinct localization and topologies (Wong et al., 2000; Sesaki et al., 2003b). l-Mgm1p is inserted in the inner membrane with a single transmembrane domain. In contrast, s-Mgm1p lacks the TM domain and is peripherally associated with both the outer and inner membranes (OMs/IMs) in the intermembrane space (IMS).

Generation of the two forms of Mgm1p is mediated by a unique sorting process called alternative topogenesis (Herlan et al., 2004). Mgm1p is synthesized in the cytosol with a presequence followed by two adjacent hydrophobic segments (TM). Mgm1p is imported into mitochondria via the translocase of the OM, and its first TM segment (TM1) is then inserted into the IM-localized TIM23 translocon. After cleavage of the presequence by the matrix-localized processing protease, one of two choices is made. In one case (Fig. 1 A, blue arrow), Mgm1p diffuses out of the TIM23 channel into the IM, forming l-Mgm1p. Alternatively (Fig. 1 A, yellow arrows), Mgm1p is further translocated into TIM23 by the action of the matrix mtHsp70 motor and the PAM complex (Herlan et al., 2004). When the second TM (TM2) reaches the IM, Mgm1p is cleaved by the rhomboid

Correspondence to Address correspondence to Hiromi Sesaki: hsesaki@jhmi.edu

H. Sesaki's present address is Department of Cell Biology, Division of Biomedical Sciences, Johns Hopkins Singapore, 31 Biopolis Way, #02-01 The Nanos, Singapore 138669.

K.A. Shepard's present address is Parallel Synthesis Technologies, Inc., 3054 Lawrence Expressway, Santa Clara, CA 95051.

Abbreviations used in this paper: IM, inner membrane; IMS, intermembrane space; mtDNA, mitochondrial DNA; OM, outer membrane; WT, wild type.

The online version of this article contains supplemental material.

The Journal of Cell Biology, Vol. 173, No. 5, June 5, 2006 651–658
http://www.jcb.org/cgi/doi/10.1083/jcb.200603092

protease Pcp1p (Herlan et al., 2003; McQuibban et al., 2003; Sesaki et al., 2003a), forming s-Mgm1p. Supporting this branched sorting pathway, pulse-chase studies show no precursor–product relationship between l-Mgm1p and s-Mgm1p (Fig. 1 B; Shepard and Yaffe, 1999). Instead, both forms of Mgm1p appear simultaneously. Here, we identify Ups1p, a novel IMS protein which regulates the sorting of Mgm1p in the topogenesis pathway and mitochondrial morphology.

Results and discussion

Ups1p regulates the steady-state level of s-Mgm1p and mitochondrial shape in a carbon source–dependent manner

To identify components required for the novel topogenesis pathway for Mgm1p, we screened yeast mutants for those with altered amounts of l- and s-Mgm1p. In particular, we examined the steady-state levels of Mgm1p in 23 yeast knockouts recently shown to have mitochondrial morphology defects (Dimmer et al., 2002; Fig. 1 B). In addition to cells lacking the protease Pcp1p, we found that knockouts of *YLR193C* showed dramatically reduced amounts of s-Mgm1p (Fig. 1 C). We named the *YLR193C* gene *UPS1* for "unprocessed". Unlike *pcp1Δ* cells, where s-Mgm1p is virtually absent, *ups1 Δ* cells contain small but detectable amounts of s-Mgm1p. Immunoblotting of isolated mitochondria showed that l-Mgm1p is located in the mitochondria of *ups1Δ* cells (Fig. 1 D). In addition, all mitochondrial proteins tested (except for the IMS protein Cyb2p) were present in similar amounts in wild-type (WT) and *ups1Δ* mitochondria. We also found that the integrity of the OM is not compromised in *ups1Δ* mitochondria in protease studies (Fig. S1 A, available at http://www/jcb.org/cgi/content/full/jcb.200603092/DC1).

Interestingly, the level of s-Mgm1p in *ups1Δ* cells varied with carbon sources. When cells were grown in the fermentable carbon source glucose (YPD), 53% of Mgm1p was converted to s-Mgm1p in WT cells. In contrast, only 1% of Mgm1p was present as s-Mgm1p in *ups1Δ* cells in YPD (Fig. 2, A and B). However, similar amounts of s-Mgm1p were found in WT (46%) and *ups1Δ* cells (47%) when grown in the nonfermentable carbon sources glycerol and ethanol (YPGE). The carbon source dependence of Ups1p for Mgm1p processing suggests that yeast cells carry a redundant Ups1p-like activity that is repressed when cells are grown on glucose. In addition to Mgm1p processing, Ups1p is also required for normal mitochondrial shape (Fig. 2, C and D) and cell growth (Fig. 2 E) in a carbon source–dependent manner. Mitochondria in *ups1Δ* cells in YPD, but not in YPGE, showed strikingly altered morphology, including fragments, short tubules, and aggregates of fragments (Fig. 2 C). These altered morphologies are similar to those seen in *pcp1* and *mgm1* mutants (Herlan et al., 2003; McQuibban et al., 2003; Sesaki et al., 2003a,b). Quantitation of mitochondrial morphology in cells grown in YPD shows that only ~25% of *ups1Δ* cells contained normal tubular mitochondria, unlike WT cells (98%) (Fig. 2 D). In contrast, in YPGE, both WT (98%) and *ups1Δ*

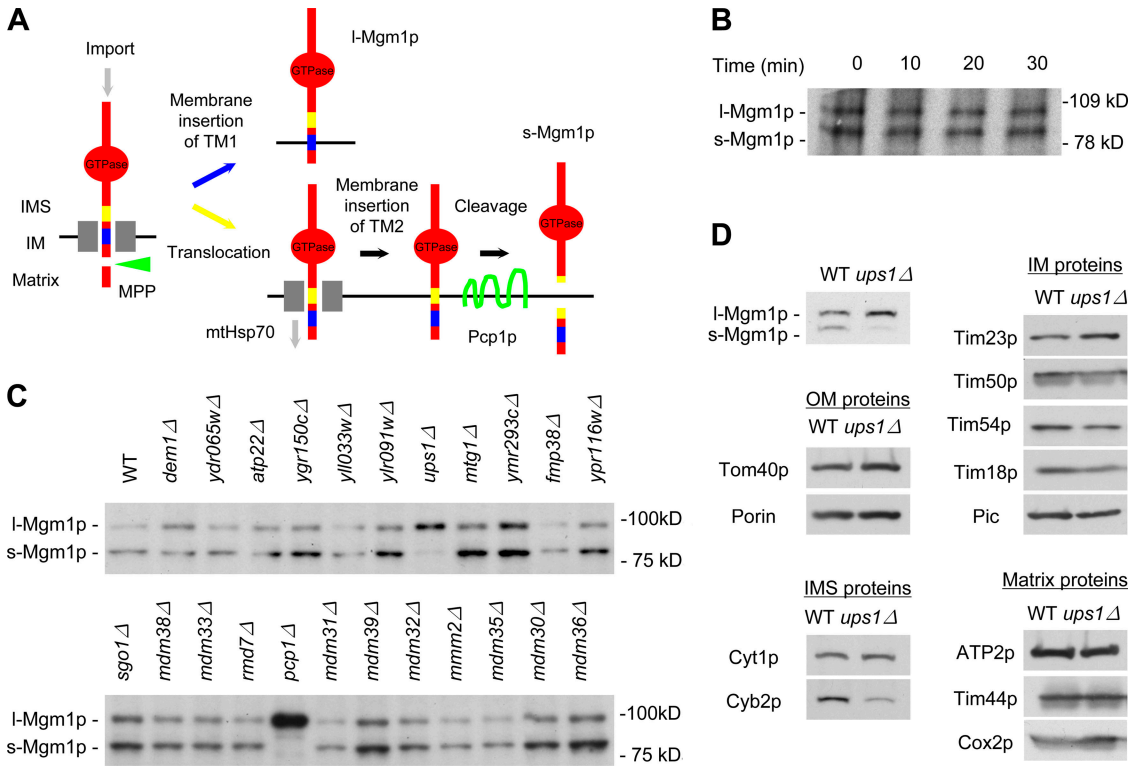

Figure 1. **Identification of *UPS1*.** (A) A model for alternative topogenesis of Mgm1p at the IM. The TIM23 translocon (gray), TM1 (blue), and TM2 (yellow) of Mgm1p, the mitochondrial processing peptidase (MPP, green) and Pcp1 protease (green) are shown. (B) WT cells were labeled with [^{35}S]-methionine and -cysteine, and chased for the indicated time period. Proteins were examined by immunoprecipitation using anti-Mgm1p antibodies. (C) Cell lysates from WT and indicated mutant strains grown in YPGalSuc were analyzed by immunoblotting using anti-Mgm1p antibodies. (D) Isolated mitochondria were analyzed by immunoblotting using the indicated antibodies.

cells (97%) contained normal mitochondrial tubules. Other organelles including the actin cytoskeleton, the ER, and vacuoles showed WT morphology in *ups1Δ* cells (Fig. S2, available at http://www/jcb.org/cgi/content/full/jcb.200603092/DC1).

Although *ups1Δ* and *pcp1Δ* cells both contain lower amounts of s-Mgm1p, there are clearly differences between the two strains. For example, although *pcp1Δ* cells lack mtDNA and are inviable on YPGE, *ups1Δ* cells contain normal mtDNA nucleoids (Fig. 2 C) and are able to grow on nonfermntable medium (Fig. 2 E). Because s-Mgmp1p is required for mtDNA maintenance (Herlan et al., 2003; McQuibban et al., 2003; Sesaki et al., 2003a), it is likely that the small but significant amounts of s-Mgm1p in *ups1Δ* cells are sufficient for mtDNA maintenance. Pcp1p has been shown to cleave another IMS protein, Ccp1p (Esser et al., 2002), and, *pcp1Δ* cells accumulated the intermediate form of Ccp1p (i-Ccp1p; Fig. 2 F). In contrast, *ups1Δ* cells contained normal amounts of the mature form of Ccp1p (m-Ccp1p; Fig. 2 F), suggesting that Ups1p specifically regulates Mgm1p processing and is not simply required for the activity of Pcp1.

Human PRELI can substitute for yeast Ups1p

UPS1 encodes a 20-kD protein (176 amino acids). Sequence analysis predicts that Ups1p contains an MSF1 domain but lacks a typical presequence and TM domain (Fig. S2). The MSF1 domain consists of ~150 residues and is named after the yeast Msf1' protein. Although Msf1'p might be involved in intramitochondrial protein sorting (Nakai et al., 1993), the exact function of Msf1'p is unknown. We found that Ups1p is homologous to multiple proteins in many organisms, from yeast to humans (Fig. 3 A and Fig. S2). In the yeast genome, Ups1p is similar to two other proteins: Msf1'p (30% identical) and Ydr185cp (30% identical). However, unlike *ups1Δ* cells, *msf1'Δ* and *ydr185cΔ* cells contained only slightly reduced amounts of s-Mgm1p (not depicted). Humans have four proteins related to Ups1p, with PREL1 showing the highest homology (31% identical; Fig. 3 A and Fig. S2). The function of PRELI is unknown, but it is highly expressed in liver, lymph node, and leukocytes (Guzman-Rojas et al., 2000) and has been localized to mitochondria (Fox et al., 2004). We found that PRELI can functionally replace Ups1p in *ups1Δ* cells. When PRELI is expressed from the constitutive *PGK1* promoter, the levels of s-Mgm1p in *ups1Δ* cells were indistinguishable from WT cells (Fig. 3 B). PRELI also rescued the mitochondrial shape defect (Fig. 3, C and D) and growth defect (Fig. 3 E) in *ups1Δ* cells. Confirming the mitochondrial location of PREL1, we found that a PREL1-GFP fusion protein colocalized with mitochondria in HeLa cells (Fig. 3 F). Our observations indicate that the function of Ups1p is evolutionarily conserved among eukaryotes.

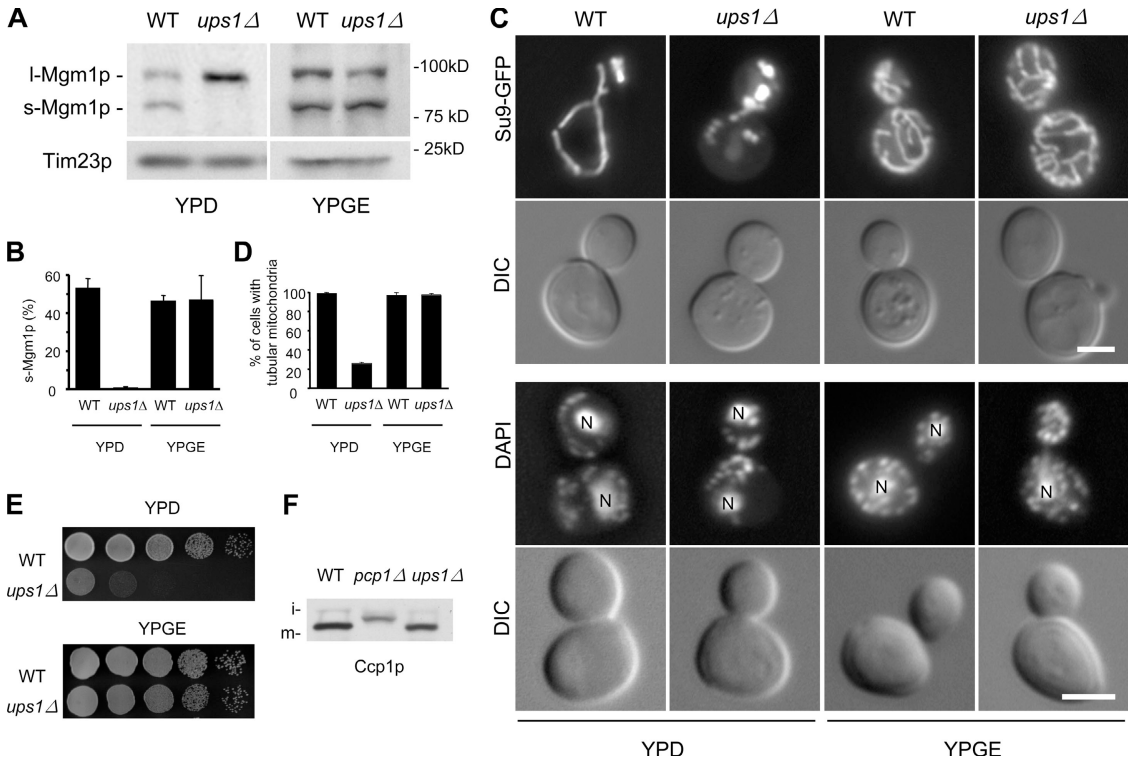

Figure 2. **Phenotypes of *ups1Δ* cells.** (A) Cell lysates from WT and *ups1Δ* cells grown in YPD or YPGE were analyzed by immnoblotting using antibodies to Mgm1p and Tim23p. (B) Mgm1p signals were quantitated by densitometry using NIH image. The percentage of s-Mgm1p was calculated from the ratio of s-Mgmp1/(s-Mgm1p + l-Mgm1p). Values are mean ± SD (n = 3). (C, top panel) Cells expressing mitochondria-targeted Su9-GFP (Westermann and Neupert, 2000) were grown in YPD or YPGE to log phase and viewed by differential interference contrast and fluorescence microscopy. (C, bottom panel) Cells were fixed in 3.7% glutaraldehyde, washed, and stained with 1 μg/ml DAPI. 'N' indicates nuclear DNA staining. Bars, 3 μm. (D) Quantitation of mitochondrial morphology (n = 300). (E) Serial dilutions of WT and *ups1Δ* cells were spotted onto YPD and YPGE and incubated at 30°C for 2 d and 4 d, respectively. (F) Lysates from cells expressing Ccp1p-HA grown in YPGalSuc were analyzed by immnoblotting using anti-HA antibodies. i: i-Ccp1p, m: m-Ccp1p.

Ups1p is associated with the mitochondrial IM in the IMS

Ups1p is peripherally associated with the outside of the mitochondrial IM. Subcellular fractionation (Fig. 4 A) and fluorescence microscopy (Fig. 4 B) show that Ups1p is associated with mitochondria. Interestingly, truncation studies showed that the first 80 residues of Ups1p, but not the first 40 residues, are sufficient for mitochondrial localization (Fig. 4 C). Protease studies demonstrated that Ups1p is located in the IMS. We found that Ups1p-myc was completely digested by trypsin treatment only after the OM was disrupted by osmotic shock, similar to the IMS-facing protein Tim23p (Fig. 4 D). In contrast, the surface receptor Tom70p was digested by trypsin in intact mitochondria. We noticed that after osmotic shock, ~50% of Ups1p-myc was associated with the mitoplast membrane (Fig. 4 E). To further characterize the membrane-bound fraction of Ups1p, mitoplasts were treated with 1.5 M sodium chloride or 0.1 M sodium carbonate (Fig. 4 F). We found that Ups1p-myc, but not the integral protein Tim23p, was completely extracted from the mitoplasts with sodium carbonate, suggesting that the association of Ups1p with membranes is peripheral. When membrane vesicles from Ups1p-myc mitoplasts were separated on sucrose gradients, Ups1p-myc cofractionated with the IM protein $F_1\beta$, but not with the OM protein porin (Fig. 4 G). Thus, Ups1p is a mitochondrial IMS protein, a half of which is peripherally associated with the IM.

We also found that Ups1p-myc is present in a protein complex of ~170 kD using blue-native gel electrophoresis of digitonin-solubilized mitochondria (Fig. 4 H). Importantly, the Ups1p complex does not contain Fzo1p, Ugo1p, Mgm1p, or Pcp1p because the size of the complex did not change in *fzo1Δ*, *ugo1Δ*, *mgm1Δ*, or *pcp1Δ* mitochondria (Fig. 4 I). We also noticed that the level of the Ups1p complex is slightly reduced in *mgm1Δ* mitochondria. This probably reflects reduced levels of Ups1p in *mgm1Δ* mitochondria (not depicted), suggesting that Mgm1p may be important for the stability of Ups1p. Furthermore, we also found no interaction of Ups1p with Fzo1p, Ugo1p, or Mgm1p in immunoprecipitation studies (not depicted).

$Mgm1_{G100D}p$ is converted to s-Mgm1p in *ups1Δ* cells

Suggesting that Ups1p functions in the sorting of Mgm1p, we find that alterations in the first hydrophobic segment of Mgm1p bypass the requirement of Ups1p for the formation of s-Mgm1p. In earlier studies, TM1 of Mgm1p was found to be critical for proper Mgm1p topogenesis (Herlan et al., 2004). When the hydrophobicity of TM1 was decreased by replacing glycine with aspartic acid ($Mgm1_{G100D}p$), TM1 was no longer efficiently arrested in the TIM23 translocon, and very little l-Mgm1p was formed. Instead, most of $Mgm1_{G100D}$ is now pulled further through the TIM23 channel, allowing access of TM2 to the Pcp1 protease; most of $Mgm1_{G100D}$ was thereby converted to s-Mgm1p

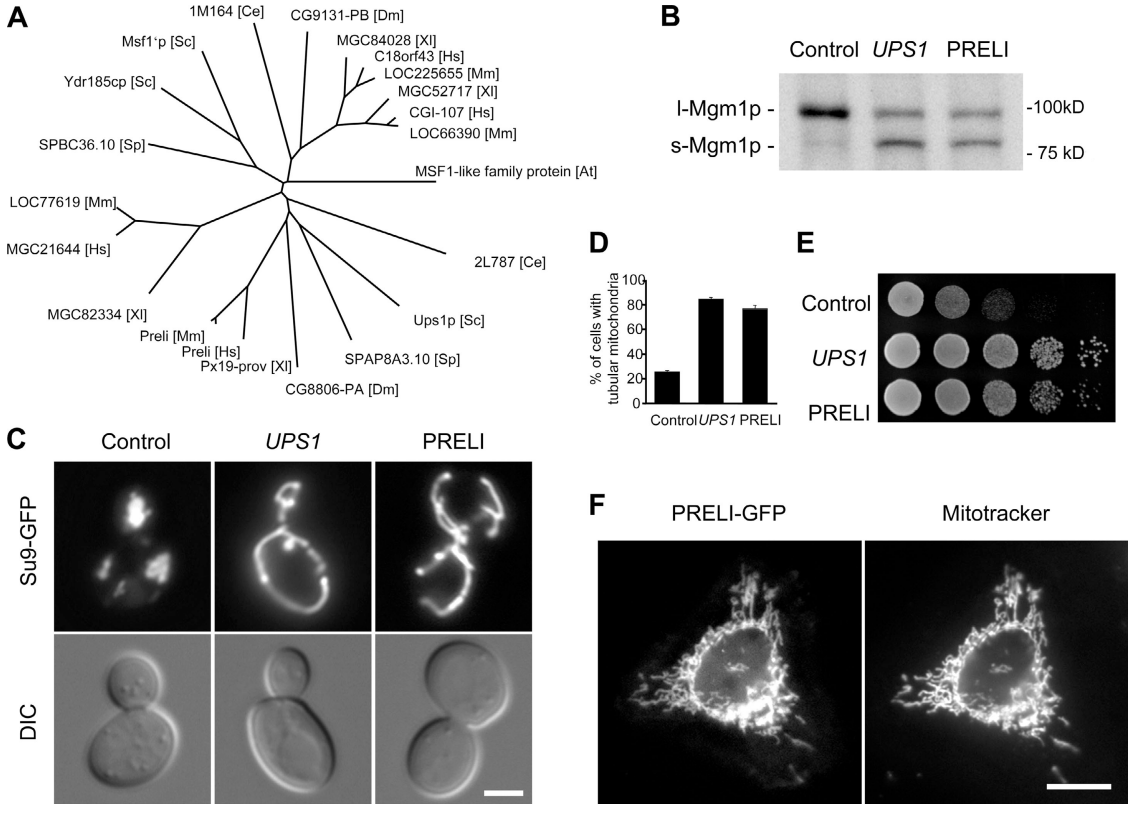

Figure 3. **The expression of PRELI rescues *ups1Δ* cells.** (A) Phylogenetic analysis of Ups1p homologues in *S. cerevisiae* (Sc), *S. pombe* (Sp), *C. elegans* (Ce), *D. melanogaster* (Dm), *X. laevis* (Xl), *M. musculus* (Mm), *H. sapiens* (Hs), and *A. thaliana* (At). (B–E) *ups1Δ* cells containing plasmids pRS314 (control), pRS314-UPS1 (UPS1), or pRS314-PRELI (PRELI) were grown in YPD. The level of Mgm1p (B), mitochondrial morphology (C and D), and growth (E) were examined as described in Fig. 2. Bar (in C), 3 μm. Values are mean ± SD in panel D. (F) HeLa cells expressing PRELI-GFP were stained with 0.1 μM Mitotracker. Bar, 10 μm.

(Fig. 5 A, lanes 1 and 2). We found that the $Mgm1_{G100D}$ alteration alleviates the need for Ups1p in the production of s-Mgm1p. As shown in Fig. 5 A (lane 3), *ups1Δ mgm1Δ* cells expressing WT Mgm1p from a plasmid contained mostly l-Mgm1p, and only a small amount of s-Mgm1p was seen. Conversely, when the $Mgm1_{G100D}$ protein was expressed in *ups1Δ mgm1Δ* cells, most of Mgm1p was converted to s-Mgm1p (Fig. 5 A, lane 4). Also arguing for a role for Ups1p in Mgm1p sorting, we found similar amounts of s-Mgm1p in *mgm1Δ* and *ups1Δ mgm1Δ* cells expressing $Mgm1_{G100D}$p (Fig. 5 A, lanes 2 and 4). Therefore, Ups1p is not simply required for the activity of Pcp1p, or for the stability of s-Mgm1p. Our results also suggest that additional substrates of Ups1p activity exist besides Mgm1p. In *ups1Δ* cells expressing $Mgm1_{G100D}$p, normal ratios of l-Mgm1p and s-Mgm1p are seen (Fig. 5 B) and Fzo1p and Ugo1p are normally expressed (Fig. 5 F), yet these cells contain fragmented mitochondria (Fig. 5, C and D) and still show growth defects (Fig. 5 E).

We found that Ups1p is not directly required for protein import into mitochondria using an in vitro import assay (Fig. S1 C). We integrated the *GAL*1 promoter in front of the *UPS1* open reading frame and isolated mitochondria from cells grown in YPD for 13 h. Immunoblotting shows that Ups1p is undetectable in the Ups1-depleted mitochondria (Fig. S1 B). In addition, the amount of s-Mgm1p is also highly reduced. Using the mitochondria, we examined protein import for Mgm1(1–228)-DHFR (Herlan et al., 2004), the matrix-targeted protein Su9-DHFR, and the IM proteins Tim22p and Tim18p. Mgm1(1–228)-DHFR consists of DHFR fused to the first 228 residues of Mgm1p, which contains two TM segments and can be cleaved by Pcp1p (Herlan et al., 2004). We found that the Ups1p-depleted mitochondria show no detectable import defect for all proteins we tested. Therefore, these data demonstrate that Ups1p is not required for mitochondrial protein import, and suggest that the processing defect for Mgm1p does not result from protein import defects. In this assay, we found similar amounts of the processed form of Mgm1(1–228)-DHFR in WT and the Ups1p-depleted mitochondria (Fig. S1 C). However, in both mitochondria the efficiency of the cleavage is considerably low (~10%; Fig. S1 C) compared with Mgm1p processing seen in vivo (~50%; Fig. 1 B). This is consistent with

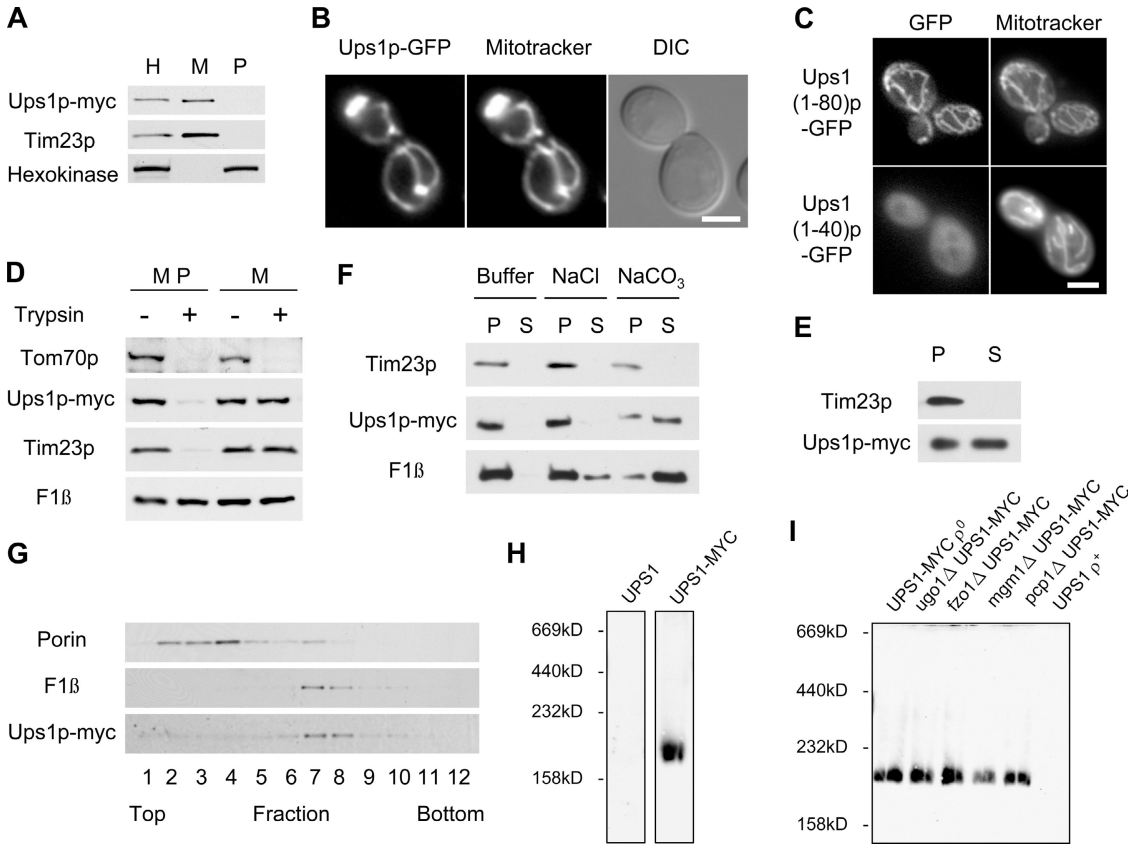

Figure 4. **Subcellular localization of Ups1p.** (A) Cells expressing Ups1p-myc were grown in YPD, homogenized (H), and separated into a mitochondrial pellet (M) and a post-mitochondrial supernatant (P) by centrifugation. Cell-equivalent amounts of each fraction were analyzed by immunoblotting with the indicated antibodies. (B) *ups1Δ* cells expressing Ups1p-GFP were stained with 0.1 μM Mitotracker. Bar, 3 μm. (C) WT cells expressing Ups1(1–80)p-GFP or Ups1(1–40)p-GFP were stained with Mitotracker. Bar, 3 μm. (D) Ups1p-myc mitochondria (M) and mitoplasts (MP) were incubated with 0.2 mg/ml trypsin for 20 min on ice and analyzed by immunoblotting. (E) The OM of Ups1p-myc mitochondria was disrupted by osmotic shock. The resulting mitoplasts were separated into supernatant (S) and pellet (P) fractions by centrifugation, and analyzed by immunoblotting. (F) Mitoplasts were pelleted by centrifugation, treated with either 1.5 M NaCl, 0.1 M Na_2CO_3, or buffer, and separated into supernatant (S) and pellet (P) fractions by centrifugation. Each fraction was analyzed by immunoblotting. (G) Ups1p-myc mitochondria were sonicated and membrane vesicles were separated on sucrose gradients. Fractions were analyzed by immunoblotting. (H and I) Mitochondria from the indicated strains grown in YPD were analyzed by blue-native electrophoresis, followed by immunoblotting.

previous observations that only a minor fraction of Mgm1p(1–228)-DHFR is processed in vitro (Herlan et al., 2004). The previous and our current studies suggest that the sorting of Mgm1p may not be a rate-limiting step in in vitro assays. It is possible that the protease activity of Pcp1p is highly reduced in these in vitro assays and becomes limiting. Supporting this idea, the mutation G_{100}→D in Mgm1p(1–228)-DHFR only slightly increases the efficiency of the processing (approximately twofold) in in vitro import assays, whereas in vivo the same mutation converts almost all Mgm1p to s-Mgm1p (Herlan et al., 2004; Fig. 5 A).

Models for Ups1p function

Our study identifies a novel IMS protein, Ups1p, which regulates the alternative topogenesis of Mgm1p. If, as our results suggest, Ups1p plays a role in Mgm1p sorting, then how does it achieve this function? In particular, how does it increase the yield of s-Mgm1p during import? In the normal sorting of Mgm1p, about half of Mgm1p arrest with TM1 in the TIM23 complex and then diffuse laterally out of the translocon into the lipid bilayer of the IM as l-Mgm1p. In one scenario, Ups1p may control the gating activity of TIM23, thus preventing all of Mgm1 from exiting the import channel, allowing some of Mgm1p to be further translocated by TIM23 and processed by Pcp1p to form s-Mgm1p. In another scenario, Ups1p may recruit or regulate the mt-Hsp70–containing PAM complex. By increasing the activity of PAM, the stop-transfer function of TM1 of Mgm1p could be countered, and more molecules could be pulled through the TIM23 complex. Arguing against these two possibilities, we find that Ups1p does not stably associate with the import machinery. Ups1p-myc is found in a complex of ~170 kD, clearly distinct from the TIM23 complex (90 kD) (Rehling et al., 2004), and Ups1p does not coimmunopreciptate with known IM import components including Tim23p, Tim50p, Tim17p, Tim21p, Pam18p, Hsp70p, and Tim44p (unpublished data). In a third scenario, Ups1p may regulate the intramitochondrial level of ATP. Consistent with this idea, inactivation of Atp6p, a subunit of F_0F_1-ATP synthase, altered the ratio of l-Mgm1p to s-Mgm1p (Herlan et al., 2004). However, the level of s-Mgm1p in the *atp6* mutants is only slightly decreased (Halern et al., 2004). Therefore, the dramatic decrease in the s-Mgm1p levels in *ups1Δ* cells cannot be explained simply by reduction in the ATP level. In addition, cells without mtDNA, thereby defective in respiration, normally produce s-Mgm1p (Fig. 5 A, lane 1). In a fourth model, Ups1p may bind directly to Mgm1 to facilitate sorting. Acting like a chaperone, Ups1p may stabilize a conformation of Mgm1p that masks the stop-transfer function of TM1. Those Mgm1 proteins bound by Ups1p would be pulled further toward the matrix and converted to s-Mgm1p. Although we found no stable interaction between Ups1p and Mgm1p, Ups1p might transiently interact with Mgm1p during the topogenesis. Additional studies are clearly needed to clarify the role of Ups1p in Mgm1p sorting.

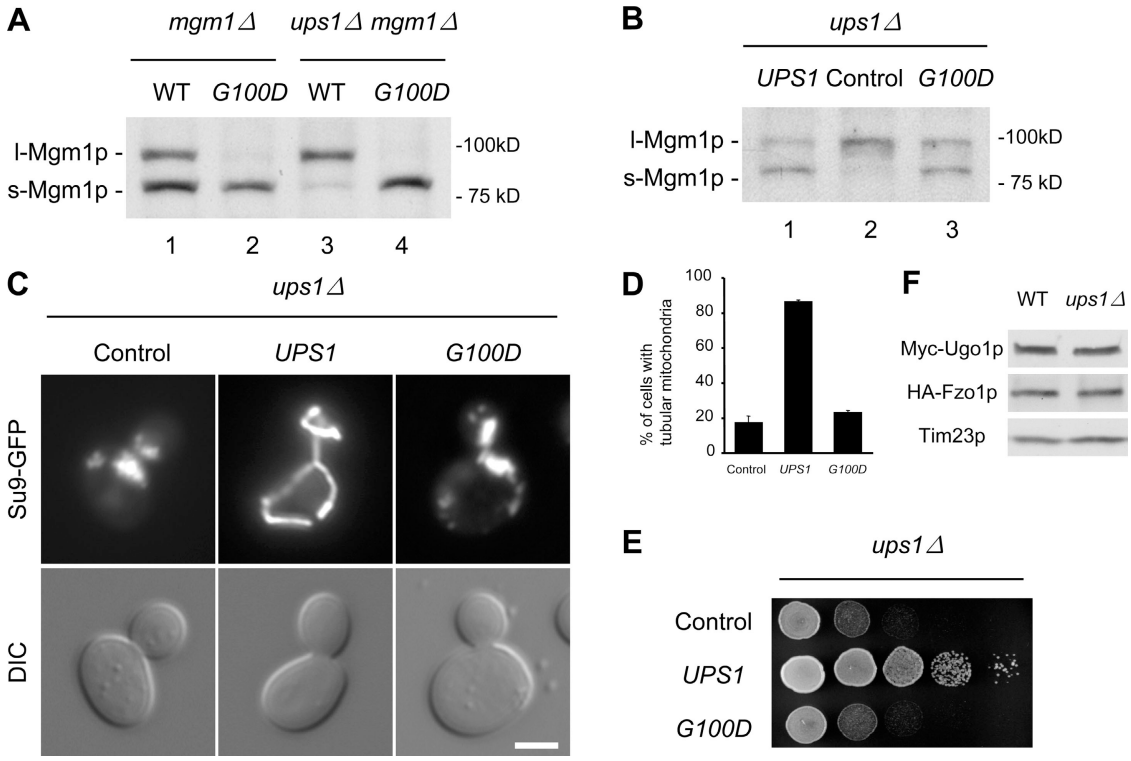

Figure 5. **Mgm1$_{G100D}$p is converted to s-Mgm1p in *ups1Δ* cells.** (A) *mgm1Δ* and *ups1Δ mgm1Δ* cells containing pRS314-*MGM1* (WT) or pRS314-*MGM1*$_{G100D}$ (G100D) were grown in YPD. The level of Mgm1p was analyzed by immunoblotting. l: l-Mgm1p, s: s-Mgm1p. (B–D) *ups1Δ* cells containing plasmids pRS314 (control), pRS314-*UPS1*, or pRS314-*MGM1*$_{G100D}$ were grown in YPD. The level of Mgm1p (B), mitochondrial morphology (C and D), and growth (E) were examined as described in Fig. 2. Bar, 3 μm. Values are mean ± SD in panel D. (F) Cell lysates were prepared from WT and *ups1Δ* cells expressing HA-Fzo1p from pHS77 (Sesaki et al., 2003b), or myc-Ugo1p from pHS57 (Sesaki and Jensen, 2001), grown in YPD, and analyzed by immunoblotting using antibodies to HA, myc, and Tim23p.

Yeast cells actively remodel their mitochondrial shape and number in response to different growth conditions and carbon sources (Jakobs et al., 2003). This plasticity is performed, at least in part, by regulated fusion and division (Jensen et al., 2000; Okamoto and Shaw, 2005). Although the precise mechanisms of l-Mgm1p and s-Mgm1p are not known, it is clear that both forms of Mgm1p are required for normal mitochondrial dynamics (Herlan et al., 2003; McQuibban et al., 2003; Sesaki et al., 2003a). By affecting the ratios of the two forms of Mgm1p, Ups1p is in an ideal position to control yeast mitochondrial shape and number. Because human PREL1 can substitute for Ups1p in Mgm1p sorting, it is likely that PREL1 normally acts on OPA1, the human homologue of Mgm1p. However, it has not been directly tested if the human rhomboid protease cleaves OPA1. Alternative topogenesis of the OPA1 isoforms may help explain the incredible diversity of mitochondrial shape, number, and distribution observed in different mammalian cell types (Karbowski and Youle, 2003; Chen and Chan, 2004).

Materials and methods

Strains, media, and genetic methods

Yeast strains used in this study are listed in Table S1. Complete disruption of the *UPS1* gene was constructed by PCR-mediated gene replacement as described previously (Brachmann et al., 1998) using the *kanMX4* gene from the pRS400 plasmid (Brachmann et al., 1998) with primers 1729 and 1730, into diploid strain FY833/844 (Winston et al., 1995). Heterozygous diploids were sporulated and dissected to obtain *ups1Δ* strains. *ups1Δ dnm1Δ* strain was constructed by crossing *MATa ups1Δ* strain and *MATα dnm1Δ* strain. *UPS1*-myc-*TRP* strain, which expresses Ups1p-myc, was constructed by homologous recombination in FY833/844 using the myc-TRP1 cassette from pFA6a-13myc-TRP1 (Longtine et al., 1998) with primers 1731 and 1732. Heterozygous diploids were sporulated and dissected to obtain *UPS1-myc* strain. *GAL1-UPS1* stain, which expresses Ups1p from the *GAL1* promoter, was constructed by homologous recombination using the kanMX6-GAL1 cassette from pFA6a-kanMX6-PGAL1 (Longtine et al., 1998) with primers 1749 and 1750. Yeast cells were grown in media including YPD (YP medium containing 2% glucose), YPGE (YP medium containing 2% glycerol and 3.2% ethanol), and YPGalSuc (YP medium containing 2% galactose and 2% sucrose). Standard genetic techniques were used (Adams et al., 1997).

Plasmids

pRS314-PRELI, a *CEN-TRP1* plasmid expressing human PRELI from the *PGK1* promoter, was constructed as follows. The *PGK1* promoter was PCR amplified from yeast genomic DNA using primers 1995 and 1996, and digested with KpnI and XhoI. Human PRELI was PCR amplified from pOTB7-PRELI (IMAGE ID 3505068; Open Biosystems) using primers 1753 and 1999, and digested with XhoI and SacII. A DNA fragment carrying the *TIM23* terminator was obtained by digesting pAA2 (Sesaki and Jensen, 2001), using SacII and SacI. The DNA fragments were subcloned into KpnI/SacII-digested pRS314.

pRS313-Su9-GFP, a *CEN-HIS3* plasmid expressing GFP fused to the presequence of subunit 9 of the F_0-ATPase of *Neurospora crassa* from the *ADH1* promoter was constructed as follows. The Su9 presequence (residues 1–69) was PCR amplified from pGEM4-Su9-DHFR using oligos 1871 and 1872. The PCR fragment was digested with EcoRI and XbaI, and cloned into EcoRI/XbaI-digested pRS313-ADH1-COX4-GFP (Sesaki and Jensen, 1999) to replace the Cox4p presequence by the Su9 presequence.

pRS314-Su9-GFP was constructed by subcloning the ADH1-Su9-GFP cassette from pRS313-Su9-GFP into pRS314 using XhoI and NotI.

To form pRS314-UPS1, a *CEN-TRP1* plasmid expressing Ups1p, *UPS1* was PCR amplified from yeast genomic DNA using primers 1727 and 1728, digested with XhoI and NotI, and cloned into pRS314.

To form pRS315-UPS1-GFP, a *CEN-LEU2* plasmid expressing Ups1p fused to GFP, *UPS1* was PCR amplified from pRS314-UPS1 using primers 1727 and 1994, digested with XhoI and NotI, and cloned into pAA1, which encodes GFP. To form truncated versions of Ups1p, primers 2060 for Ups1p(1–80) and 2061 for Ups1(1–40)p were used instead of 1994.

To form pRS314-MGM1$_{G100D}$, glycine at residue 100 of pRS314-Mgm1p (Sesaki et al., 2003b) was replaced by aspartic acid using site-directed mutagenesis according to manufacturer's instructions (QuickChange; Stratagene).

pSP6-MGM1(1–228)-DFHR was constructed as described previously (Herlan et al., 2004).

Cell lysates

Cell lysates were prepared as described previously (Herlan et al., 2003). In brief, cells (1 OD_{600} unit) at log phase were collected by centrifugation and washed in buffer A (2 mM EDTA, 2 mM PMSF, 100 μM TPCK, and protease inhibitor cocktail; Sigma-Aldrich). Cells were resuspended in 500 μl of buffer A, and 100 μl of lysis buffer (1.85 M NaOH and 106 mM β-mercaptoethanol) was added. After incubation for 10 min on ice, 316 μl of 100% TCA was added. Samples were incubated for 15 min on ice, washed twice with acetone, resuspended in 50 μl SDS-PAGE sample buffer, and boiled for 5 min. Proteins (8.3 μl per lane) were analyzed by SDS-PAGE and immunoblotting.

Antibodies

Antibodies raised against the COOH-terminal 10 amino acids of Mgm1p (Sesaki et al., 2003b) were affinity purified against the same peptide using SulfoLink Coupling Gel (Pierce Chemical Co.) according to the manufacturer's instructions. Antiserum to Ups1p was produced using the peptide corresponding to residues 162–175 (FVIQKLEEARNPQF) and affinity purified against the same peptide as described above.

Pulse-chase analysis

WT cells were grown in minimal medium lacking methionine and cysteine to log phase. Cells were harvested, resuspended in 40 mM KPi, pH 6.0, and 1% glucose, and labeled for 5 min at 30°C in the presence of 0.1 mCi/ml [^{35}S]Translabel (MP Biomedicals). The chase was initiated by adding unlabeled methionine and cysteine to 20 μM. Cells were collected and processed for immunoprecipitation as described previously (Shepard and Yaffe, 1999).

Blue-native gel electrophoresis

600 μg of mitochondria were resuspended on ice in 96 μl of 50 mM NaCl, 5 mM 6-aminocaproic acid, 100 mM Bis Tris, pH 7.0, 50 μg/ml α2 macroglobulin, and protease inhibitor cocktail (Sigma-Aldrich). Then, 24 μl of 10% digitonin was added, and mitochondria were solubilized for 15 min. After centrifugation at 12,500 *g* for 10 min, 165 μg of mitochondrial proteins was separated on 6–16% acrylamide gradient gels (Schagger and von Jagow, 1991).

Expression of PRELI-GFP in HeLa cells

HeLa cells were grown in DME (Invitrogen) with 10% fetal calf serum (Atlanta Biologicals). The open reading frame of PRELI was PCR amplified from pOTB7-PRELI using oligos 1753 and 1760, digested with XhoI and EcoRI, and subcloned into XhoI/EcoRI-digested pEGFP-N1. (CLONTECH Laboratories, Inc.). 4×10^5 HeLa cells were transfected with 1 μg pPRELI-GFP using Lipofectamine (Life Technologies, Inc.) following the manufacturer's directions.

Microscopy

Yeast cells were observed using a microscope (Axioskop; Carl Zeiss MicroImaging, Inc.) with a 100× Plan-Neofluar objective. Fluorescence and differential interference contrast images were captured with a CCD camera (Orca ER; Hamamatsu) using OpenLab software version 3.0.8 (Improvision, Inc.). HeLa cells were viewed using a microscope (Axiovert; Carl Zeiss MicroImaging, Inc.) with a 40× Achrostigmat objective. Images were captured with a Photometrics CoolSNAP camera (Roper Scientific) using IPLab software (Scanalytics).

Imports into isolated mitochondria

Mitochondria were isolated from WT and *GAL1-UPS1* strains and examined for protein import as described previously (Ryan et al., 2001).

Immunoprecipitatation

Immunoprecipitation was performed as described previously (Sesaki and Jensen, 2004), except that 1% digition was used instead of Triton X-100.

Online supplemental material

Fig. S1 shows that Ups1p is not required for the integrity of the OM, for protein import into mitochondria, and for the morphology of actin cytoskeleton, the ER and vacuoles. Fig. S2 shows that Ups1p is evolutionarily

conserved among eukaryotes. Table S1 shows yeast strains and PCR primers used in this study. Online supplemental material is available at http://www/jcb.org/cgi/content/full/jcb.200603092/DC1.

We thank K. Cerveny, M. Youngman, S. Studer, and A. Aiken Hobbs for exciting discussions and critically reading the manuscript.

This work is supported by National Institutes of Health grants to R.E. Jensen (GM46803) and to M.P. Yaffe (GM44614), and an American Heart Association grant to H. Sesaki (0465498U).

Submitted: 20 March 2006
Accepted: 3 May 2006

References

Adams, A., D. Gottschling, C. Kaiser, and T. Stearns. 1997. Methods in Yeast Genetics. Cold Spring Harbor Laboratory Press, Plainview, NY. 177 pp.

Alexander, C., M. Votruba, U.E. Pesch, D.L. Thiselton, S. Mayer, A. Moore, M. Rodriguez, U. Kellner, B. Leo-Kottler, G. Auburger, et al. 2000. OPA1, encoding a dynamin-related GTPase, is mutated in autosomal dominant optic atrophy linked to chromosome 3q28. *Nat. Genet.* 26:211–215.

Brachmann, C.B., A. Davies, G.J. Cost, E. Caputo, J. Li, P. Hieter, and J.D. Boeke. 1998. Designer deletion strains derived from *Saccharomyces cerevisiae* 288C: a useful set of strains and plasmids for PCR-mediated gene disruption and other applications. *Yeast.* 14:115–132.

Chen, H., and D.C. Chan. 2004. Mitochondrial dynamics in mammals. *Curr. Top. Dev. Biol.* 59:119–144.

Delettre, C., G. Lenaers, J.M. Griffoin, N. Gigarel, C. Lorenzo, P. Belenguer, L. Pelloquin, J. Grosgeorge, C. Turc-Carel, E. Perret, et al. 2000. Nuclear gene OPA1, encoding a mitochondrial dynamin-related protein, is mutated in dominant optic atrophy. *Nat. Genet.* 26:207–210.

Dimmer, K.S., S. Fritz, F. Fuchs, M. Messerschmitt, N. Weinbach, W. Neupert, and B. Westermann. 2002. Genetic basis of mitochondrial function and morphology in *Saccharomyces cerevisiae*. *Mol. Biol. Cell.* 13:847–853.

Esser, K., B. Tursun, M. Ingenhoven, G. Michaelis, and E. Pratje. 2002. A novel two-step mechanism for removal of a mitochondrial signal sequence involves the mAAA complex and the putative rhomboid protease Pcp1. *J. Mol. Biol.* 323:835–843.

Fox, E.J., S.A. Stubbs, J. Kyaw Tun, J.P. Leek, A.F. Markham, and S.C. Wright. 2004. PRELI (protein of relevant evolutionary and lymphoid interest) is located within an evolutionarily conserved gene cluster on chromosome 5q34-q35 and encodes a novel mitochondrial protein. *Biochem. J.* 378:817–825.

Guzman-Rojas, L., J.C. Sims, R. Rangel, C. Guret, Y. Sun, J.M. Alcocer, and H. Martinez-Valdez. 2000. PRELI, the human homologue of the avian px19, is expressed by germinal center B lymphocytes. *Int. Immunol.* 12:607–612.

Herlan, M., C. Bornhovd, K. Hell, W. Neupert, and A.S. Reichert. 2004. Alternative topogenesis of Mgm1 and mitochondrial morphology depend on ATP and a functional import motor. *J. Cell Biol.* 165:167–173.

Herlan, M., F. Vogel, C. Bornhovd, W. Neupert, and A.S. Reichert. 2003. Processing of Mgm1 by the rhomboid-type protease Pcp1 is required for maintenance of mitochondrial morphology and of mitochondrial DNA. *J. Biol. Chem.* 278:27781–27788.

Jakobs, S., N. Martini, A.C. Schauss, A. Egner, B. Westermann, and S.W. Hell. 2003. Spatial and temporal dynamics of budding yeast mitochondria lacking the division component Fis1p. *J. Cell Sci.* 116:2005–2014.

Jensen, R.E., A.E. Aiken Hobbs, K.L. Cerveny, and H. Sesaki. 2000. Yeast mitochondrial dynamics: fusion, division, segregation, and shape. *Microsc. Res. Tech.* 51:573–583.

Jones, B.A., and W.L. Fangman. 1992. Mitochondrial DNA maintenance in yeast requires a protein containing a region related to the GTP-binding domain of dynamin. *Genes Dev.* 6:380–389.

Karbowski, M., and R.J. Youle. 2003. Dynamics of mitochondrial morphology in healthy cells and during apoptosis. *Cell Death Differ.* 10:870–880.

Longtine, M.S., A. McKenzie III, D.J. Demarini, N.G. Shah, A. Wach, A. Brachat, P. Philippsen, and J.R. Pringle. 1998. Additional modules for versatile and economical PCR-based gene deletion and modification in *Saccharomyces cerevisiae*. *Yeast.* 14:953–961.

McQuibban, G.A., S. Saurya, and M. Freeman. 2003. Mitochondrial membrane remodelling regulated by a conserved rhomboid protease. *Nature.* 423:537–541.

Nakai, M., T. Takada, and T. Endo. 1993. Cloning of the YAP19 gene encoding a putative yeast homolog of AP19, the mammalian small chain of the clathrin-assembly proteins. *Biochim. Biophys. Acta.* 1174:282–284.

Okamoto, K., and J.M. Shaw. 2005. Mitochondrial morphology and dynamics in yeast and multicellular eukaryotes. *Annu. Rev. Genet.* 39:503–536.

Rehling, P., K. Brandner, and N. Pfanner. 2004. Mitochondrial import and the twin-pore translocase. *Nat. Rev. Mol. Cell Biol.* 5:519–530.

Ryan, M.T., W. Voos, and N. Pfanner. 2001. Assaying protein import into mitochondria. *Methods Cell Biol.* 65:189–215.

Schagger, H., and G. von Jagow. 1991. Blue native electrophoresis for isolation of membrane protein complexes in enzymatically active form. *Anal. Biochem.* 199:223–231.

Sesaki, H., and R.E. Jensen. 1999. Division versus fusion: Dnm1p and Fzo1p antagonistically regulate mitochondrial shape. *J. Cell Biol.* 147:699–706.

Sesaki, H., and R.E. Jensen. 2001. UGO1 encodes an outer membrane protein required for mitochondrial fusion. *J. Cell Biol.* 152:1123–1134.

Sesaki, H., and R.E. Jensen. 2004. Ugo1p links the Fzo1p and Mgm1p GTPases for mitochondrial fusion. *J. Biol. Chem.* 279:28298–28303.

Sesaki, H., S.M. Southard, A.E. Hobbs, and R.E. Jensen. 2003a. Cells lacking Pcp1p/Ugo2p, a rhomboid-like protease required for Mgm1p processing, lose mtDNA and mitochondrial structure in a Dnm1p-dependent manner, but remain competent for mitochondrial fusion. *Biochem. Biophys. Res. Commun.* 308:276–283.

Sesaki, H., S.M. Southard, M.P. Yaffe, and R.E. Jensen. 2003b. Mgm1p, a dynamin-related GTPase, is essential for fusion of the mitochondrial outer membrane. *Mol. Biol. Cell.* 14:2342–2356.

Shepard, K.A., and M.P. Yaffe. 1999. The yeast dynamin-like protein, mgm1p, functions on the mitochondrial outer membrane to mediate mitochondrial inheritance. *J. Cell Biol.* 144:711–720.

Westermann, B., and W. Neupert. 2000. Mitochondria-targeted green fluorescent proteins: convenient tools for the study of organelle biogenesis in *Saccharomyces cerevisiae*. *Yeast.* 16:1421–1427.

Winston, F., C. Dollard, and S.L. Ricupero-Hovasse. 1995. Construction of a set of convenient *Saccharomyces cerevisiae* strains that are isogenic to S288C. *Yeast.* 11:53–55.

Wong, E.D., J.A. Wagner, S.W. Gorsich, J.M. McCaffery, J.M. Shaw, and J. Nunnari. 2000. The dynamin-related GTPase, Mgm1p, is an intermembrane space protein required for maintenance of fusion competent mitochondria. *J. Cell Biol.* 151:341–352.

Wong, E.D., J.A. Wagner, S.V. Scott, V. Okreglak, T.J. Holewinske, A. Cassidy-Stone, and J. Nunnari. 2003. The intramitochondrial dynamin-related GTPase, Mgm1p, is a component of a protein complex that mediates mitochondrial fusion. *J. Cell Biol.* 160:303–311.